Polydomain-monodomain transition in nematic elastomers

S. V. Fridrikh and E. M. Terentjev
Cavendish Laboratory, University of Cambridge, Madingley Road, Cambridge CB3 0HE, United Kingdom
(Received 17 February 1999)

Director textures and alignment of polydomain nematic elastomers under uniaxial extension are described theoretically applying the concept of randomly quenched disorder introduced by network cross-links. Within this model, treated with the replica trick and Gaussian variational approximation, the polydomain-monodomain transition occurs in a critical fashion with a small jump and rapid increase of the macroscopic order parameter. The transition is characterized by a plateau on the stress-strain curve. The critical stress value at which the transition takes place is estimated as $\sim \mu Q_{ch}$ with μ the rubber modulus of the elastomer and Q_{ch} the parameter of chain anisotropy. The aligning of polydomain texture occurs via rotation of domains rather than their growth, with domain size almost unchanged through and above the transition. Experimental data obtained by several groups for various nematic elastomers are analyzed, showing a qualitative agreement with model predictions. [S1063-651X(99)06908-1]

PACS number(s): 64.70.Md, 75.10.Nr, 83.80.Dr

I. INTRODUCTION

All liquid crystalline (nematic) polymers and elastomers usually show the presence of a polydomain director texture observed as a ''Schlieren texture'' under the crossed polarized optics [1]. This appears to be a universal feature leading to strong scattering of light from the optical contrast between regions of different director orientation. The correlation length of local nematic alignment (domain size) in this macroscopically distorted state is normally of the order of few microns. These structures always occur after cooling the system below the nematic to isotropic transition temperature T_{NI} and in many cases are stable and reversible, at least in elastomers, indicating the fact that in this highly disordered state the system is at its equilibrium. On the other hand, ordinary liquid crystals, which also possess the ''Schlieren texture'' after cooling below T_{NI} quickly coarsen, increasing the domain size and eliminating most of the defects, thus achieving a uniform nematic director alignment, see [2], for instance.

Why do elastomers and many polymers not follow the same pattern of coarsening? The reason could be in the very long relaxation time of defects in these systems. In ordinary liquid crystals all topological defects are mobile and can be annealed very quickly. In nematic polymers the annealing of the defects will be affected by a much higher viscosity and, indeed, one may expect a very slow dynamics of relaxation. On the other hand, long polymers may possess defects in their chemical structure (e.g., chain branching or impurities), which may never be annealed. In case of elastomers the main source of defects is the network crosslinks themselves, which are quenched in the network during the synthesis and are not able to relax. In this paper we are describing the properties of a nematic system affected by such quenched sources of orientational disorder.

Other liquid crystalline systems with random disorder include the nematic in pores of silica gels [3], polymer-stabilized and polymer-dispersed liquid crystals, e.g., Ref. [4]. The source of the random disorder in such cases is the surface anchoring of nematic director on the walls of the random porous matrix on a length scale similar, or greater than the characteristic period of resulting director textures. In nematic elastomers the random disorder arises from defects in the polymer network structure and cross-links quenched during the synthesis, on a much smaller length scale which allows for coarse-graining and continuum description.

The behavior of many other systems such as spin glasses and vortices in superconductors is strongly influenced by the presence of randomly quenched disorder. In spin glasses, randomly distributed and oriented impurity atoms give easy directions for the magnetization. This favors the magnetization vector to be locally parallel to randomly oriented easy axes given by the impurities, however, the average macroscopic magnetization is zero. Similarly, in vortex arrays in superconductors, the long distance order is lost due to the distortions in the lattice caused by randomly quenched impurities.

The progress in understanding statistical properties of systems with quenched disorder is based on the concept of weak disorder when the distance between two defects is much less than the resulting correlation length of the structure [5,6]. It is not obvious that this type of modeling is applicable in case of nematics in porous media where one deals with the difficult case of strong discrete sources of disorder. On the other hand, in nematic elastomers the typical distance between the sources of disorder is of the order of few nanometers, while the correlation length is in the micron range. Thus this system possesses a weak random field and can be more naturally described by continuous model. Regardless of the theoretical modeling, both systems show complex dynamic behavior typical of random systems characterized by slow (logarithmic) relaxation [7,8].

One of the main features of systems with weak quenched disorder, well understood within continuum models, is that the long-range order is preserved only at distances less than the correlation length ξ_D [5–9]. For instance, if one cross-links nematic polymer above the nematic-isotropic transition temperature T_{NI}, the junction points create local sources of anisotropy, which will be randomly oriented in space. Cooling such a system into the nematic state will then give rise to

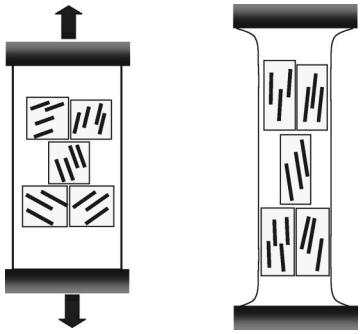

FIG. 1. Polydomain nematic elastomer aligning under the uniaxial extension.

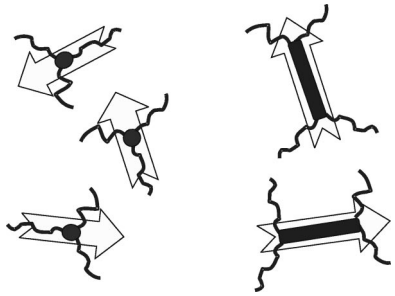

FIG. 2. The schematic representation of typical network crosslinks possessing some anisotropy and giving the easy nematic ordering direction.

the weak random field which destroys the alignment at large distances. The system exists in a ''polydomain'' state with correlation length (domain size) ξ_D typically of the order of few microns. The correlation loss at large distances arises from the competition between the aligning effect of Frank elasticity and the disordering effect of local sources. This can be illustrated by the Imry-Ma argument [6] discussed below. Thus the ground state of macroscopic director texture in any system with even weak random disorder is ''glassy,'' i.e., similar to spin glasses.

As the correlation length is close to the light wavelength, the polydomain director field strongly scatters the light, including multiple scattering in thick samples. When such ''polydomain'' nontransparent nematic elastomer, Fig. 1(a), is subjected to a uniaxial extension, it undergoes a polydomain-monodomain (P-M) transition manifested by the rapid increase of macroscopic nematic alignment in a sample [Fig. 1(b)] and is accompanied by a spectacular plateau on a stress-strain curve.

This peculiar behavior of polydomain nematic elastomers under uniaxial stress has been observed in many experiments on a variety of materials [10–18]. The common features of this effect are the following: (i) One observes a linear (Hookean) stress-strain relation at low deformations, before the transition threshold is reached; (ii) a stress plateau (an almost constant stress for a range of deformations) is encountered at medium strains, then followed by the stress growth at higher strains, see Figs. 6; (iii) the sample, opaque before stretching, becomes transparent ''monodomain'' when passing through the stress plateau region.

The question of universality of this P-M transition then arises and requires an appropriate theoretical model. In this paper we present such a theory accounting for many features of the P-M transition. We bring together experimental data obtained by several groups and analyze them with the model predictions, finding, where possible, the model parameters from fitting the data extracted from the corresponding publications. This paper is organized as follows. Section II presents a basic description of random field model and main theoretical predictions that emerge from it. Section III reviews the experimental data and gives an example of analysis in terms of the model. In the Sec. IV we summarize the results and also discuss the limitations of the model.

II. POLYDOMAIN-MONODOMAIN TRANSITION

A. Quenched disorder and polydomains

To understand the physics of P-M transition we start from studying the physical origin and the role of coarse-grained weak random field in creating the original equilibrium polydomain state. We consider nematic elastomer with randomly distributed impurities and crosslinks which impose local easy anisotropy axes. Such a material can be obtained by cross-linking nematic polymer in isotropic phase, which will quench the orientation of anisotropic cross-links and defects of the network structure. The typical network junctions always possess some degree of local anisotropy and on subsequent cooling into nematic phase they will interact with surrounding mesogenic molecular units, forcing them to be parallel to the long axis of the cross-link in its immediate vicinity. The strength or this cross-link-to-nematic order coupling is characterized by the random energy constant γ. Due to the quadrupolar symmetry of the problem, this coupling may be described by the following term in the free energy,

$$F_{rf} = -\sum_i \frac{\gamma}{2}[\mathbf{k}_i \cdot \mathbf{n}(\mathbf{R}_i)]^2, \tag{1}$$

where $\mathbf{k}_i$ is the unit vector along the axis of ith cross-link, $\mathbf{R}_i$ is the position of this cross-link, and $\mathbf{n}(\mathbf{R}_i)$ is the local nematic director, Fig. 2. The summation in Eq. (1) is carried over all such local sources of anisotropy. We then coarse-grain this by introducing a continuum cross-link density $\rho(\mathbf{r}) = \Sigma_i \delta(\mathbf{r} - \mathbf{R}_i)$, which imposes a completely random orientation of an easy anisotropy axis $\mathbf{k}(\mathbf{r})$.

For reasons of mathematical simplicity it is convenient to take the nematic ordering and random anisotropy axes both confined to the x-y plane, though being dependent on all three spatial coordinates (this corresponds to $3d$ XY model in spin systems, $n=2$, $d=3$). This choice does not seem to affect the results qualitatively [19] but substantially simplifies the analysis. The local coarse-grained nematic ordering is changing the direction slowly, so that the director $\mathbf{n} = \{\cos\theta, \sin\theta\}$ is parametrised by a single angle θ with $|\mathbf{n}| = \text{const}$. This choice, in fact, corresponds to most experiments where a thin flat strip of elastomer was subjected to deformations and the (planar) director distribution examined by optical or x-ray scanning through the film.

When many defects are randomly distributed in space one can assume their density to have a Gaussian distribution:

$$P[\rho] \simeq \exp\left\{ -\int d^3 r \frac{\rho^2}{2\rho_0} \right\}, \tag{2}$$

where ρ_0 is the mean density of impurities, see for instance [20]. As the defects are at the same time randomly oriented in the x-y plane, we have the probability of their orientation $P[\mathbf{k}]=1/2\pi$.

In the continuum theory, any deviation of nematic director from a uniform orientation is penalized by Frank elasticity. The random field energy, presented in a discrete form in (1), can now be written in a coarse-grained continuous form via the crosslink density $\rho(\mathbf{r})$,

$$F_{Fr}+F_{rf}=\int d^3r\left\{\frac{K}{2}(\nabla\mathbf{n})^2-\frac{\gamma}{2}\rho(\mathbf{k}\cdot\mathbf{n})^2\right\}, \qquad (3)$$

where K is Frank elasticity constant in one-constant approximation.

The free energy containing these two terms, F_{Fr} and F_{rf}, captures the main features of systems with quenched weak orientational disorder and one can now apply the Imry-Ma argument [6]. For a texture with the correlation distance ξ_D we can estimate the gradient $\nabla\mathbf{n}$ as $\sim 1/\xi_D$, immediately getting an estimate for the Frank energy (per domain of the size ξ_D): $F_{Fr}\sim KV\xi_D^{-2}$, or $F_{Fr}\sim K\xi_D^{d-2}$, where V and d are the domain volume and the dimensionality of the system. In the usual three dimensions, $F_{Fr}\sim K\xi_D$. The number of random defects N in such a domain is proportional to the domain volume ξ_D^d, $N\simeq\rho_0\xi_D^d$. To minimize the free energy the system will tend to have nematic director parallel to the direction most of the cross-links (vectors $\mathbf{k}$) within this volume are parallel to. To visualize this picture, one can take all $\mathbf{k}_i$ and make a chain from them by connecting them head to tail. The end-to-end vector of such a ''chain'' will give the preferable alignment direction for the nematic director. The mean square length of this end-to-end vector will be proportional to $N^{1/2}\simeq\rho_0^{1/2}\xi_D^{d/2}$ as in the case of any random walk. This value indicates the magnitude of the mean field of quenched sources, averaged over the chosen domain volume. Thus the excess of the crosslinks looking in the preferable direction will be of the order of $N^{1/2}$ and the system will gain the random-field energy of the order of $F_{rf}\sim\gamma(\rho_0\xi_D^d)^{1/2}$ by aligning in this direction. Hence the domain free energy F_D can be estimated as:

$$F_D\simeq K\xi^{d-2}-\rho_0^{1/2}\gamma\xi^{d/2}$$

or

$$F_D\simeq K\xi-\rho_0^{1/2}\gamma\xi^{3/2} \quad \text{for} \quad d=3. \qquad (4)$$

Minimizing F_D with respect to the correlated domain size ($\partial F_D/\partial\xi_D=0$) we obtain the characteristic length $\xi_D\sim K^2/\rho_0\gamma^2$ for $d=3$. This simple scaling argument shows that no matter how weak is the random disorder it will win at sufficiently long distances and destroy the long range ordering breaking the system into the correlated regions of size ξ_D.

B. Continuum nematic rubber elasticity

In the case of nematic elastomers one should also deal with nontrivial elasticity of a nematic rubber network. The rubber elasticity is of an entropic origin and the elastic energy of polymer network is controlled by the end-to-end distribution of the network chains. In case of the ordinary isotropic rubber the chains have spherical shapes at equilibrium and any deformation will change the elastic energy via changing the chains shape and, therefore, their conformational freedom.

In nematic rubber, polymer chains forming the network are anisotropic and in most cases have the average shape of uniaxial prolate ellipsoid, the nematic director being parallel to the long axis of the ellipsoid. The rotation of the nematic director will change the sample shape without change in the chains average ellipsoidal shape and, consequently, without change in elastic energy. It literally means that certain deformations accompanied by the director rotations are soft, i.e., take place at no energy cost. A good example of such a deformation, important for understanding of P-M transition, is the shear of an aligned nematic rubber perpendicular to the director. Under such a shear, the chains may rotate their undeformed ellipsoidal shapes (i.e., rotate the nematic director) thus accommodating the extension, but necessarily in combination with the simple shear, and keep their conformational entropy and resulting rubber-elastic energy constant. This deformation will be soft till the director is rotated by 90° and the system is no more able to accommodate deformation by the director rotation, see [21,22] for details. Olmsted [23] has shown that there exists a continuous set of soft deformations, which by appropriately combining strains and director rotations can make the elastic response vanish.

The existence of soft deformations gives rise to several peculiar effects in mechanical behavior of nematic rubbers, some of which are explained on the basis of the neoclassical theory of rubber elasticity [21], providing a general expression for the free energy of the nematic rubber valid for large deformations. For the purposes of this paper and for the reasons of mathematical simplicity it is sufficient to consider small strains $\varepsilon_{\alpha\beta}$ and to expand the free energy up to the terms quadratic in $\varepsilon_{\alpha\beta}$. The qualitative form of such an expansion was envisaged a long time ago by de Gennes [24]. Later, the molecular expressions for elastic constants were obtained by Olmsted [23]. We make a further simplification and describe the director-network coupling by a single term $-UQ_{\alpha\beta}\varepsilon_{\alpha\beta}$, as it was done in [25], with $Q_{\alpha\beta}=Q_N(n_\alpha n_\beta-\frac{1}{3}\delta_{\alpha\beta})$ the nematic order parameter and U the constant of coupling between the nematic ordering and elastic deformations. Molecular theory [21] and the experiment [26] give the order of magnitude for U, which is the same as the rubber elastic modulus μ, i.e., $U\simeq\mu\sim 10^5$ J/m^3 in a typical rubber.

The free energy change F_{mech} in monodomain nematic elastomer due to mechanical deformation characterized by stress and strain tensors $\sigma_{\alpha\beta}$ and $\varepsilon_{\alpha\beta}$ can than be presented as the following [25]:

$$F_{mech}=\int d^3r\left[\frac{\mu}{2}\varepsilon_{\alpha\beta}\varepsilon_{\alpha\beta}-\sigma_{\alpha\beta}\varepsilon_{\alpha\beta}-UQ_{\alpha\beta}\varepsilon_{\alpha\beta}\right]. \qquad (5)$$

Minimizing F_{mech} with respect to the strain $\underline{\underline{\varepsilon}}$ we obtain the equilibrium value of the mechanical free energy $F_{mech}(\varepsilon^*)$. (A more complete derivation of the effective nematic energy and an accompanying discussion can be found in, for instance, in [27,28]. Here we use a cruder approach simply to illustrate the symmetry of stress-director coupling and the estimate of its energy scale.)

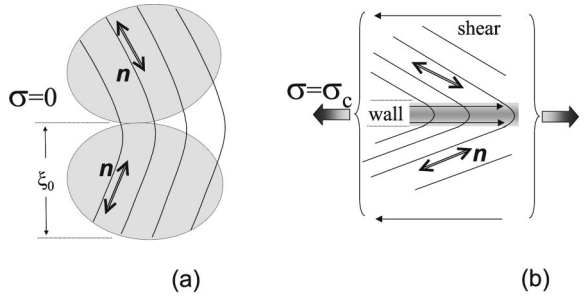

FIG. 3. Nematic elastomer structure in two neighboring domains: (a) no external stress, (b) at the transition point. Note the uniaxial extension turning into shear with opposite directions in neighboring domains and the domain wall localization.

$$F_{mech}(\varepsilon^*)=\int d^3r\frac{1}{2\mu}[\sigma_{\alpha\beta}\sigma_{\alpha\beta}+U^2Q_{\alpha\beta}Q_{\alpha\beta} -2UQ_{\alpha\beta}\sigma_{\alpha\beta}]. \tag{6}$$

The first term in (6) is the (constant) mechanical energy of an applied stress, the second term will simply shift the temperature of nematic to isotropic transition in proportion to the network crosslinking density ρ_0. They are independent of the director field configuration $\mathbf{n}(\mathbf{r})$ and are thus irrelevant to our problem of director textures (we shall assume that the local nematic order parameter Q_N remains constant far from T_{NI}). The third term describes the orientational effect of stress. In the case of uniaxial extension caused by the stress σ parallel to, say, z-axis it will turn into $(Q_NU/\mu)\sigma(n_zn_z-1/3)$. After dropping the irrelevant constant we finally obtain the correction to the free energy of a monodomain nematic elastomer under uniaxial extension dependent on the director field configuration, coupled to the stress $\underline{\underline{\sigma}}$:

$$\Delta F_{mech}=\int d^3r\left[-\frac{Q_NU}{\mu}\sigma(\hat{\mathbf{s}}\cdot\mathbf{n})^2\right], \tag{7}$$

where $\hat{\mathbf{s}}$ is the unit vector parallel to the extension axis. This coupling carries the simple (and expected) message: the nematic director tends to be aligned along the uniaxial extension axis.

However, one should take into account an additional elastic energy due to polydomain structure of elastomer. As the correlated spin glass, the zero-stress disordered elastomer does not have pronounced interfaces between correlated regions. The director changes smoothly in space, without making sharp bends, gradually loosing the memory of its orientation. Nevertheless, when an external stress is applied, the system would minimize the elastic energy if the director field and elastic network deformations are separated in space. Namely, by localizing the director distortions in narrow domain walls, the system will make the domains free of director undulations and allow them to be deformed softly. Such domain walls localization causes transformation of uniaxial extension of the whole sample into shear deformation of single domains with shear direction alternating between different domains (see Fig. 3 and [18]).

Localizing the deformation inside the domain walls will cost some additional energy and will be energetically favorable only above certain threshold. This energy and related

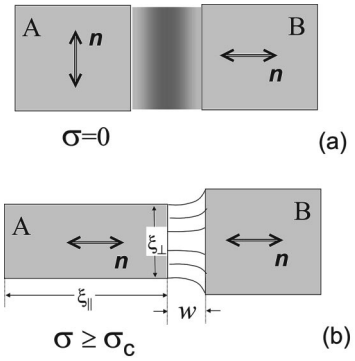

FIG. 4. Two neighboring domains (a) before and (b) after the transition. The director in the domain A is rotated by 90° creating the size mismatch in the domains boundary region of width w.

deformations can be estimated using the following scaling argument. Let us consider two neighboring domains with initially perpendicular director orientations, shown schematically in Fig. 4(a). Under the extension ε, the domain B will generate the elastic energy of the order of

$$\frac{\mu}{2}\varepsilon^2\xi^3,$$

in proportion to its volume ξ^3. The wall region of the width w will be deformed as well, with the corresponding elastic penalty

$$\frac{\mu}{2}\varepsilon^2\xi^2w.$$

However, the domain A may be able to deform softly, with director rotating by up to 90°, with no elastic energy raised in its volume. The mismatch between the two domains [the difference between their natural dimensions along and across $\mathbf{n}$, Fig. 4(b)] will cause additional deformation $\tilde{\varepsilon}$ inside the domain wall which can be estimated as $(\xi_\parallel-\xi_\perp)/\xi \simeq(\ell_\parallel/\ell_\perp-1)$, with $\xi_\parallel$ and $\xi_\perp$ the domain dimensions along and across the local nematic director. The aspect ratio (anisotropy) of nematic polymer chains $r=\ell_\parallel/\ell_\perp$ is reflected in the local shape of the network and provides the geometric mismatch, see Fig. 4(b). Hence the additional strain in domain walls is $(\xi/w)(\ell_\parallel/\ell_\perp-1)$ and the corresponding energy cost in the wall of volume ξ^2w is

$$\mu/2w\xi^4(\ell_\parallel/\ell_\perp-1)^2.$$

.

Thus the mechanical free energy per unit volume of a polydomain nematic elastomer with weak random disorder and under uniaxial extension can be expressed as:

$$\Delta F=\frac{\mu}{2}\varepsilon^2\frac{w}{\xi}+\frac{\mu}{2w}\frac{(\ell_\parallel/\ell_\perp-1)^2}{\xi}+\frac{\mu}{2}\varepsilon^2. \tag{8}$$

The first part in Eq. (8) favors the smaller width w, thus allowing more volume to be taken by the soft domain A. The second part has the opposite effect, tending to increase the width w over which the newly generated size mismatch has to be accommodated. Optimizing Eq. (8) with respect to w gives for the equilibrium domain wall width:

$$w^*=\frac{\xi}{\varepsilon}(\ell_\parallel/\ell_\perp-1), \tag{9}$$

decreasing with the growing applied strain ε. Note that the chain anisotropy ($\ell_\parallel/\ell_\perp - 1$) is due to the coupling between the polymer backbone and the mesogenic groups and, thus, is proportional to the nematic order parameter Q_N. Substituting Eq. (9) into Eq. (8), we obtain an additional energy term $\approx \mu\varepsilon(\ell_\parallel/\ell_\perp - 1)$ responsible for the localisation of domain walls. This energy density, linear in macroscopic strain, should be added to the external stress term $-\sigma\varepsilon$, providing the value of effective stress $\tilde{\sigma} \approx \sigma - \mu(\ell_\parallel/\ell_\perp - 1)$. As we shall see later, this shift determines the value of the threshold stress for the *P-M* transition. Finally, the free energy of a polydomain nematic elastomer under uniaxial extension is

$$F = \int d^3r \left[\frac{K}{2}(\nabla \mathbf{n})^2 - \frac{\gamma}{2}\rho(\mathbf{r})(\mathbf{k}\cdot\mathbf{n})^2 - u(\sigma - \sigma_w)(\hat{\mathbf{s}}\cdot\mathbf{n})^2 \right], \tag{10}$$

where $\sigma_w \simeq \mu(\ell_\parallel/\ell_\perp - 1)$ and the dimensionless coupling constant $u = (Q_N U)/\mu$.

C. Polydomain-monodomain transition

From the above discussion it follows that drastic changes in the elastic behavior and ordering in nematic elastomers happen at a certain value of external stress when correlated domains start deforming softly and the walls between them become narrow. The director rotation associated with this soft deformation of the domains with initially misaligned director leads to the growth of a long range order in the system. At the same time, the reduction in the rubber elastic response produces a stress plateau. When this *P-M* transition is completed, the system is in the aligned monodomain state, which is responding with a normal rubber-elastic energy to a further extension. The range of the deformation ε where the director rotation takes place roughly corresponds to the soft plateau on the typical stress-strain plot.

A number of questions on the state of the system just after and further above the transition arise: (i) what is the critical stress value corresponding to the transition, (ii) how ordered is the system just after the transition, (iii) how does the long range (macroscopic) alignment in the system evolve on further increase in stress above the transition. To answer these questions we have developed a theory, evaluating the equilibrium state of a system described by the Hamiltonian Eq. (10), briefly reported in [29]. The theory uses the replica trick [30] to deal with the quenched random fields $\rho(x)$ and $\mathbf{k}(x)$ and approximates the resulting complicated Hamiltonian by means of the Gaussian variational method (GVM) [31,32] using $H = \Sigma_q \frac{1}{2} G^{-1}(q)\theta_q\theta_{-q}$ as a trial Hamiltonian with $G^{-1}(q)$ the replica-symmetric variational ansatz to $\langle \theta_q \theta_{-q} \rangle$. This approximate way of solving the problem is inadequate in the zero-field disordered spin-glass like system [31,32], but is valid for relatively high values of external stress above the threshold, $u(\sigma - \sigma_w) \gg K/\xi_D^2 \sim 10$ J/m^3.

From GVM we have for the average values of the director normal modes $\langle |\theta(q)|^2 \rangle$:

$$\frac{V}{kT}\langle |\theta(q)|^2 \rangle = \frac{1}{Kq^2 + D} + \frac{\omega K^2}{kT\xi_0 (Kq^2 + D)^2}, \tag{11}$$

where D is a variational parameter used in GVM, ξ_0 is the domain size at zero external stress, $\omega = \exp\{-2kTq_{max}/(\pi^2 K)\}$ is a constant of the order of one, q_{max} being the upper cutoff in reciprocal space, $q_{max} \simeq 2\pi/a$, with a the size of a mesogenic molecular unit. This result is a generalization of one obtained by Larkin [7] for vortices in superconductors with no external fields (which corresponds to D equal to zero). The first term in (11) corresponds to thermal disorder, the second one—to random disorder. The variational parameter D plays the role of mass and suppresses fluctuations due to both thermal and quenched disorder. The nonzero mass penalizes otherwise unbound long wavelength fluctuations and limits their amplitude.

As was shown before [29], in the absence of stress the replica symmetry is broken and the trivial replica-symmetric solution with $D = 0$ is stable only within the correlated domain length scale. It means that the long distance order in the system is lost and the ground state of the system is polydomain. The nontrivial replica-symmetric solution with nonzero D describing the state of the system with long range order exists only for external stresses above the critical value σ_c. From the equation connecting variational parameter D with the modified stress $\tilde{\sigma} = \sigma - \sigma_w$ [29]:

$$D = 2u\omega^{1/2}\tilde{\sigma}\exp\left\{ -\frac{\pi K^{1/2}}{4\xi_0 D^{1/2}} \right\}, \tag{12}$$

we obtain the value of the critical stress σ_c (and the modified threshold $\tilde{\sigma}_c = \sigma_c - \sigma_w$) and of the corresponding effective mass D_c:

$$\sigma_c = \mu(\ell_\parallel/\ell_\perp - 1) + \frac{\pi^2 e^2}{128\omega^{1/2}u}\frac{K}{\xi_0^2}, \tag{13}$$

$$D_c = \frac{\pi^2 K}{64\xi_0^2}, \tag{14}$$

where, recall, the coupling constant $u = Q_N U/\mu$ and the zero-stress domain size is $\xi_0 \approx 16\pi^2 K^2/\omega\rho_0\gamma^2$. The second term on the right hand side of (13) arises from the balance between the random field and Frank elasticity and gives a very low value of the threshold. (The similar balance produces a threshold value of external magnetic field aligning the weakly disordered spin glass, $H_c \sim (\rho_0\gamma^2)^2/K^3$, see [19,29].) It can be estimated suggesting typical values for $K \sim 10^{-11}$ N, $\xi_0 \sim 10^{-6}$ m, $\mu \sim U \sim 10^5$ Pa, and the nematic order parameter $Q_N \sim 1$. Then $\tilde{\sigma}_c$ should be of the order of $1-10$ Pa, a very small value comparing with the assumed rubber energy scale μ. In contrast, the first term in (13) arises from the rubber elasticity and the domain wall localization, and is of the order of $\mu(10^5$ Pa), i.e., much bigger than $\tilde{\sigma}_c$. Thus nematic rubber elasticity accompanied by the domain walls localization causes a strong increase in the threshold stress for *P-M* transition. As an estimate for the threshold stress we can take simply:

$$\sigma_c \approx \mu(\ell_\parallel/\ell_\perp - 1) \sim \mu Q_{ch} \tag{15}$$

with the nematic polymer backbone anisotropy characterized by a ''chain order parameter'' Q_{ch}.

From Eq. (11) the macroscopic order parameter $S_{\rm macro} = Q_N(1/V)\int d^3r\langle 2\cos(\theta)-1\rangle$ can be estimated. This parameter is experimentally accessible by several standard techniques and is of particular importance here. We have for $S_{\rm macro}$:

$$S_{\rm macro} \simeq Q_N \exp\left\{ -\frac{kTq_{max}}{\pi^2 K}\left[1 + \frac{\omega\rho_0\gamma^2}{16kTD^{1/2}K^{1/2}q_{max}} \arctan\left(\frac{K^{1/2}q_{max}}{D^{1/2}} \right) \right] \right\}. \tag{16}$$

Taking $K \simeq kT/a \simeq kTq_{max}/2\pi$ we can estimate the jump of the long distance order at the transition point $S_{\rm macro}(\sigma_c)$:

$$S_{\rm macro}(\sigma_c) \simeq Q_N \exp\left\{ -\frac{2}{\pi}(1+2\pi) \right\} \sim 0.01 Q_N, \tag{17}$$

which is really small. The behavior of $S_{\rm macro}$ above the transition is described by Eq. (16). Just above the critical stress D has a square-root singularity, giving a slow growth of S_{macro} with increasing the stress: $\Delta S_{macro}(\tilde{\sigma}) \sim \exp\{(\tilde{\sigma} - \tilde{\sigma}_c)^{1/2}\}$. However, the replica-symmetry approximation used to obtain our Eqs. (11)–(16) is unreliable in the immediate vicinity of the critical point, at $\tilde{\sigma} - \tilde{\sigma}_c \sim K/\xi_0^2 \sim 10$ J/m^3. On the other hand, the experimental resolution of stress is usually too low to examine this region in detail. Thus, this initial growth in the long distance order will rather be seen as an apparent jump in S_{macro} at the transition point.

At $\tilde{\sigma}_c \ll \tilde{\sigma} \ll Kq_{max}^2 \sim 10^7$ J/m^3, which corresponds to the realistic experimental values of stress, the long distance order grows fast with increasing stress and approaches the saturation value:

$$S_{\rm macro}(\tilde{\sigma}) \simeq s_o + (Q_N - s_o)\exp\left\{ -\frac{K^{1/2}}{2\omega^{1/2}u^{1/2}\xi_0(\sigma-\sigma_c)^{1/2}} \right\}, \tag{18}$$

where the small constant s_o accounts for the ''apparent jump'' at the vicinity of the transition point which is not described by the approximate Eq. (18). At $\tilde{\sigma} \to \infty$ $S_{\rm macro}$ tends to Q_N, the thermodynamic value of nematic order parameter in a fully aligned elastomer.

It is interesting to know what happens with correlation length (which we called the domain size) at and above the transition. The answer can be obtained from Eq. (11) [29]. The real-space correlation function $B(x) = \langle[\theta(x) - \theta(0)]^2\rangle$, characterizing the decrease of the correlations with distance, will be strongly affected by the stress only if we have big value of the effective mass D, namely $D \sim Kq_{max}^2$. In reality, we find that at the transition point $D_c \sim K/\xi_0^2$, at reasonably high stresses $D \sim \mu \sim 10^5$ J/m^3, both being well below Kq_{max}^2. Thus the condition of small D is satisfied at and well above the transition the domain size ξ_D is not strongly affected by the stress. The evolution of the polydomain state through and above the transition, therefore, proceeds via the reorientation of correlated regions towards the field direction, while keeping their characteristic size unchanged in the first approximation.

III. ANALYSIS OF THE EXPERIMENTAL RESULTS

The P-M transition was investigated by several experimental groups in a variety of nematic elastomers, both main-chain and side-chain. Various experimental techniques have been used to characterize their mechanical behavior and long range liquid crystalline ordering: stress-strain measurements, x-ray scattering, IR dichroism measurements, light scattering, and polarized optical microscopy.

The polymers investigated are characterized by different values of polymer chain anisotropy ($\ell_\parallel/\ell_\perp - 1$) controlling the transitional behavior. The difference in the chain anisotropy arises from different degrees of coupling between the nematic order of mesogenic groups and the polymer backbone. In case of main-chain elastomers the anisotropy of the chain Q_{ch} together with that of the mesogens Q_N is high below T_{NI}. The experiment [33] reports $\ell_\parallel/\ell_\perp \geqslant 10$ in a main-chain system, obtained from the direct neutron scattering data. In side-chain elastomers, due to the weak coupling between the backbone and pending mesogenic groups, the chain anisotropy is usually small (e.g., $\ell_\parallel/\ell_\perp \sim 1.1$ in polyacrylates [13]) even when the mesogens are strongly ordered. The materials investigated can be divided into four groups in the order of the decreasing chain anisotropy: (i) main-chain epoxy elastomers [Fig. 5(a)] with chain anisotropy, $\ell_\parallel/\ell_\perp \sim 5-10$, (ii) polysiloxane side-chain elastomers [Fig. 5(b)] with $\ell_\parallel/\ell_\perp \sim 2.5$ [34], (iii) polyacrylate elastomers with T-shaped side groups [Fig. 5(c)] with $\ell_\parallel/\ell_\perp \sim 1.8$ [10] and

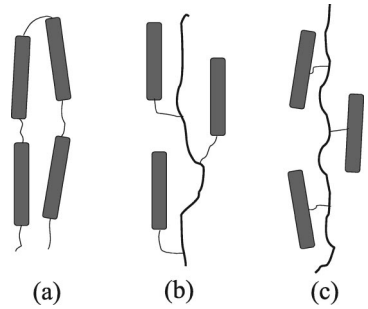

FIG. 5. The main types of the nematic polymer chain architecture: (a) semiflexible main-chain nematic polymers, (b) conventional side-chain nematic polymer, (c) T-shaped side-chain nematic polymers (see text for detail).

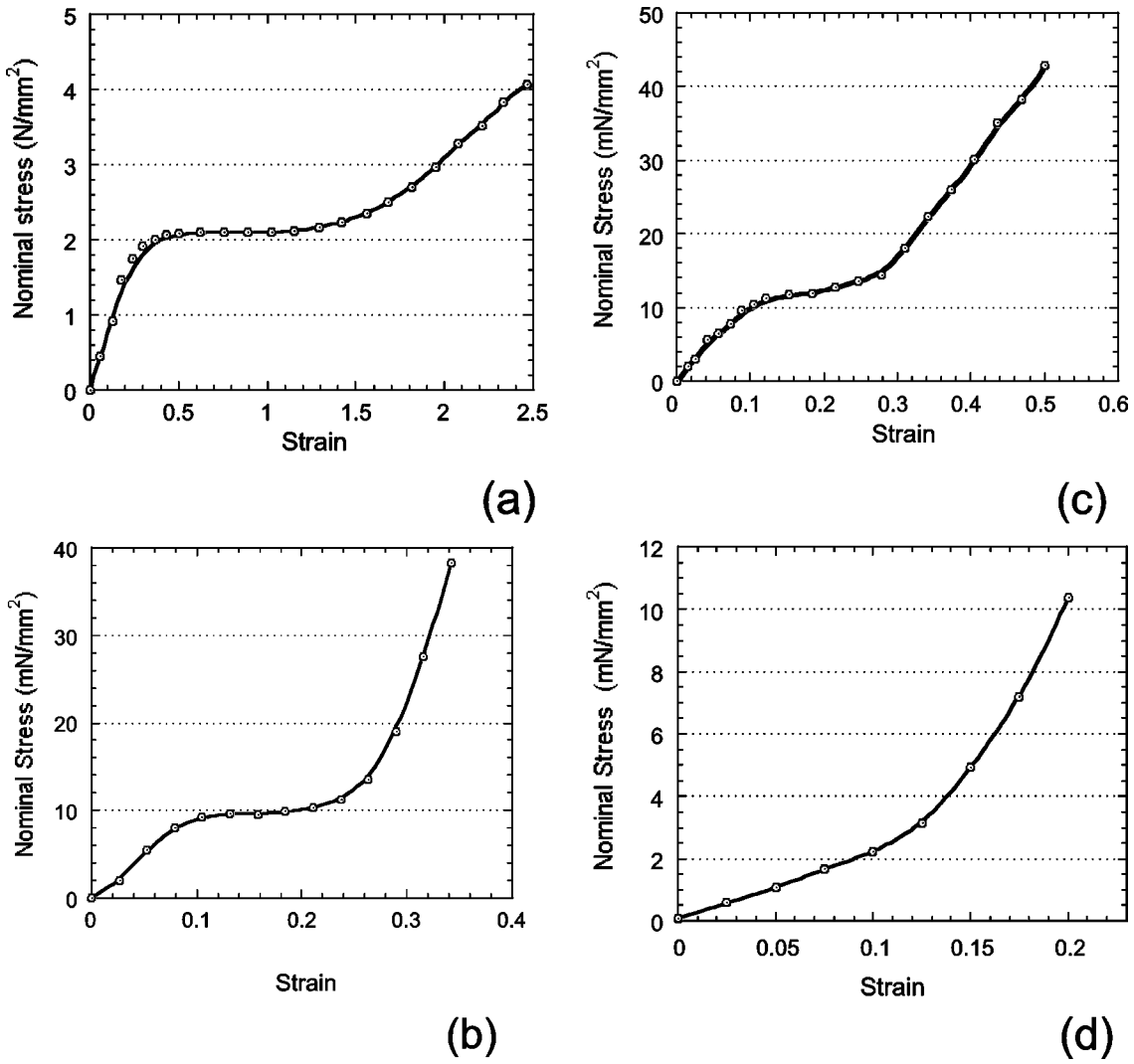

FIG. 6. Stress-strain curves for polydomain nematic elastomers: (a) main-chain epoxy elastomers (data points from Fig. 11 of [15]), (b) side-chain siloxane elastomers (data points from Fig. 2 of [18]), (c) acrylic side-chain elastomers (data points from Fig. 3 of [10]), (d) acrylate backbone elastomer with cyanobiphenyl side groups (data points from Fig. 6 of [13]).

(iv) polyacrylate side-chain elastomers [Fig. 5(b)] with $\ell_\parallel/\ell_\perp \sim 1.1$ [13].

A. Threshold stress

One of the main signatures of the transition, namely, the presence of the threshold stress with the plateau on the stress-strain curve, was clearly observed in all the materials with considerable chain anisotropy [(i)–(iii)] [10,11,14–16,18], but was reported to be very small if at all noticeable in side-chain elastomers based on polyacrylate backbone [12,13], see Fig. 6. The value of the threshold stress $\sigma_c \simeq \mu(\ell_\parallel/\ell_\perp - 1)$ is controlled by the chain anisotropy and rubber elastic modulus. Hence, even for the same elastic modulus μ, the difference in the threshold stress values due to the different values of $\ell_\parallel/\ell_\perp$ would be noticeable. Thus the predicted threshold stress value should be proportional to the rubber shear modulus: $\sigma_c \simeq (0.1-1)\mu$. This is in agreement with experimental reports. Ortiz *et al.* present the data for main-chain epoxy elastomers: $\sigma_c = 2.0\times 10^6$ Pa, $\mu = 4.4\times 10^6$ Pa ($\sigma/\mu = 0.45$) [15]. Clarke *et al.* reported for polysiloxane side-chain elastomers: $\sigma_c = 1.1\times 10^4$ Pa, $\mu = 1.0\times 10^5$ Pa ($\sigma/\mu = 0.11$) [18]. The results of Finkelmann *et al.* for side-chain elastomers with acrylic backbone and a variety of side-group mesogens show $\sigma_c = 1.2\times 10^4$ Pa, $\mu = 1.0\times 10^5$ Pa ($\sigma/\mu = 0.12$) [10]. Finally, the results of Talroze *et al.* [13] register no threshold for the *P-M* transition in polyacrylate rubbers, which is not unexpected since $\mu = 5\times 10^4$ Pa and $\ell_\parallel/\ell_\perp$ is very low.

B. Soft stress plateau

The value of strain λ_m corresponding to the end of the plateau and the beginning of the monodomain regime can give an independent idea of the chain anisotropy. For a crude estimate, assume that at $\lambda = 1$ (no deformation) the average size of the polydomain sample is affinely proportional to $l = (\ell_\parallel \ell_\perp^2)^{1/3}$ due to the random orientation of the aligned nematic regions. At the end of the stress plateau the domains completed the rotation and the director is mostly parallel to the strain direction. The sample size at this strain should be proportional to $\ell_\parallel$ giving $\lambda_m \simeq \ell_\parallel^{2/3}/\ell_\perp^{2/3}$, or $\ell_\parallel/\ell_\perp \simeq \lambda_m^{3/2}$. One should expect λ_m to decrease with growing temperature when $Q_{ch} \to 0$ and $\ell_\parallel \to \ell_\perp$, thus decreasing the width of the

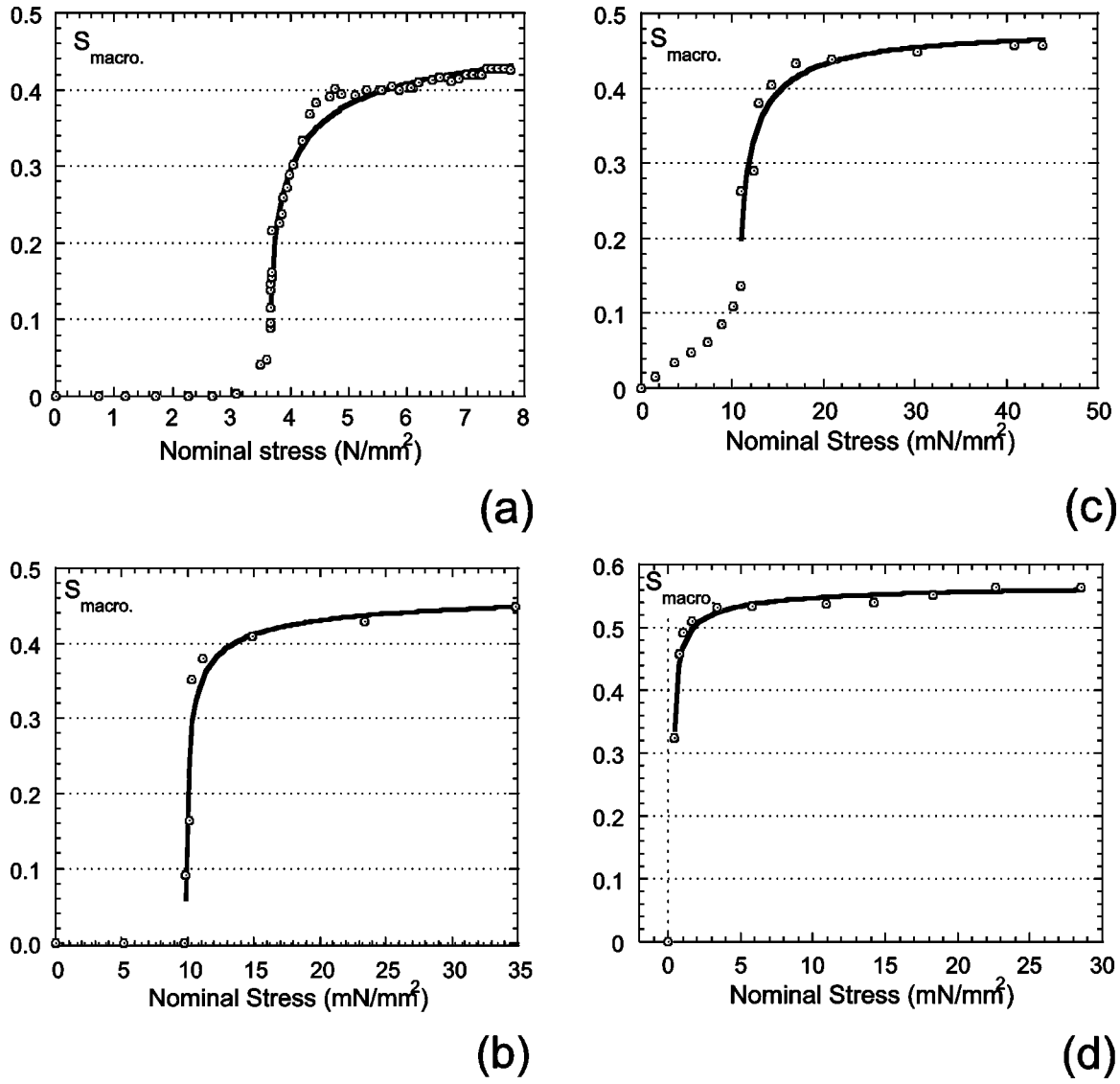

FIG. 7. Macroscopic order parameter as a function of applied stress. Letters refer to the same systems as in Fig. 6: (a) data from Fig. 12 in of [14], (b) data from Fig. 7b of [18], (c) data from Fig. 9 of [10], (d) data from Fig. 2b of [13]. The curves show the fitting with the model prediction Eq. (18).

plateau, which is in agreement with experimental results for several side-chain elastomers [10,18]. One should also expect the threshold stress value σ_c to decrease with increasing temperature, again due to the decrease in the backbone chain anisotropy. This prediction is not readily confirmed by experimental results for side-chain elastomers, which show the threshold stress roughly independent on temperature [10,18], but it is in agreement with the data for the main-chain elastomers [16].

Nematic elastomers obtained by chemical and γ-radiation cross-linking of acrylate backbone with cyanobiphenyl mesogenic side groups are known for very small chain anisotropy [13]. They show no visible threshold stress. Similarly they show no visible plateau, although one may interpret a sharp increase in the stress-strain slope at around $\lambda-1=\varepsilon=0.03-0.08$ as the point where the *P*-*M* transition ends [Fig. 6(d)]. This brake point is shifting to higher strains with decrease in the temperature, similar to λ_m, possibly indicating the end of the domain rotation. From there onwards the film is optically transparent and the material is an aligned monodomain. The value of strain corresponding to the completion of the transition in these systems is considerably smaller than that in the other systems described above, confirming the suggestion about the role of the low chain anisotropy.

C. Mean orientation parameter

Together with stress-strain characterization, the measurements of the macroscopic order parameter can be made, as a function of applied stress. These data may be obtained either by IR-dichroism measurements [10] or by the x-ray scattering technique [13,18]. All the curves for $S_{\mathrm{macro}}(\sigma)$ show rapid increase at the transition point which may be interpreted as a small jump, given the experimental error. This is followed by an increase and saturation at the level of $S_{\mathrm{macro}} \simeq 0.3-0.6$ depending on the material and temperature, Fig. 7.

The theoretical model, Eqs. (16) and (18) and Ref. [29], makes very similar predictions. A small apparent jump at the

threshold $s_o \leqslant 0.1$ should be treated as a fitting parameter. The evolution of mean orientation parameter $S(\sigma)$ just above the threshold, and at high stresses follows the asymptotic equation (18): $S_{\mathrm{macro}}(\sigma \geqslant \sigma_c) \propto \exp(-K^{1/2}/2\omega^{1/2}u^{1/2}\xi_0\tilde{\sigma}^{1/2})$.

Equation (18) can be used to fit experimental data. Both Q_N and σ_c are not fitting parameters, but can be read off the experimental plots. Assuming the domain size $\xi \sim 2.5\mu m$ (as reported in [16,18]) and thus obtaining $\sqrt{K/4\omega u}$ from the fitting in Figs. 7, we can deduce the values for the Frank constant K: for all materials $K \sim 10^{-12}$ N which is close to the values reported in the literature [35] $K = 10^{-12} - 10^{-11}$ N.

However, the systems behave differently before the onset of *P-M* transition. The early experiment has shown that in the case of side-chain acrylic elastomers the long range alignment is slowly growing at very low stresses below the transition [10] [Fig. 6(c)], while there is no noticeable macroscopic alignment before the onset of the transition in siloxane based side-chain elastomers [18] [Fig. 6(b)]. Slight increase in the long range order prior to the abrupt *P-M* transition was also reported for main-chain elastomers [16] [Fig. 6(a)]. The theoretical model presented here does not cover the behavior of the system below the transition (at $\sigma < \sigma_c$) and does not give any predictions for the long distance order in this region. One of the possible reasons for this growth may come from inhomogeneities in the material when some domains experience higher stress than the others and start aligning at a lower value of the average stress.

D. Domain size and the random field strength

Another important prediction of the theory is the weak dependence of the correlation length (domain size) ξ_D on the external stress through and above the transition $\xi_D \approx 150K^2/\rho_0\gamma^2$. This was confirmed experimentally for side-chain elastomers with siloxane backbone by light scattering measurements [18]. The scattering patterns obtained for the samples during and above the transition have a characteristic cross shape with the peak positions in the stretching direction and across it corresponding to the dimensions of slightly anisotropic domains (correlated regions) giving $\xi_\parallel \sim 2.5$ μm and $\xi_\perp \sim 2.2$ μm. The peaks change their positions very little during the extension and fade gradually as the long distance order is imposed and the director nonuniformities are suppressed, thus decreasing the optical contrast.

The domain size as a function of stress and strain in main chain elastomers was investigated by Ortiz *et al.* [16] by polarized optical microscopy. They observe the domains to become elongated in the stretching direction and the domain sizes along and across the stretching direction $\xi_\parallel$ and $\xi_\perp$ to grow with increasing strain. Initially (before stretching) the reported values are $\xi_\parallel \approx \xi_\perp \sim 2.5$ μm. After the *P-M* transition $\xi_\perp$ grows very little: less than twice for very high strains ($\varepsilon = 200\%$), reaching $\xi_\perp \sim 4$ μm. The domain size along the stress axis $\xi_\parallel$ increases 3–5 times, however, showing no sign of divergence. All these observations confirm the idea that domains are present in the material at any stress and that the long distance order is established via their reorientation, not via their growth.

We are now in a position to estimate the strength of the effective random field γ, a parameter of the model. For $K \sim 10^{-12}$ N, one obtains $\rho_0\gamma^2 \sim 6 \times 10^{-17}$ J^2/m^3. On the other hand, we estimate the crosslink density ρ_0 from the rubber modulus $\mu \sim \rho_0 kT$, at room temperature $\rho_0 \sim 2.5 \times 10^{25}$ m^{-3}. This gives the estimate for the coupling constant $\gamma \sim 1.5 \times 10^{-21}$ J$\sim 0.4kT$. This is not an unreasonable value for the coupling of an individual crosslink, see Eq. (1). Such estimates are only possible well below the nematic-isotropic transition. At $Q_N \to 0$ both K and γ should rapidly decrease and the variation of their ratio, giving the domain size ξ, cannot be predicted from the present model.

IV. SUMMARY

The *P-M* transition in nematic elastomers in external mechanical field brings the system from the orientational texture of glassy ''polydomain'' with no macroscopic alignment to a ''monodomain'' state where the long distance alignment is well established. The further stretching of the sample suppresses the variations of nematic director at the micron scale and the material becomes optically transparent.

Due to the coupling between the rubber elasticity and polymer chains anisotropy the system possesses the property of soft elasticity which allows for certain deformations to develop without an elastic energy cost. Under the uniaxial stress the system finds a way of saving the free energy by separating the director field distortions and polymer network deformation in space. Localization of director distortions in the domain walls formed under applied stress allows the domains to become more pronounced, homogeneous, and to undergo a soft deformation. Thus the uniaxial extension of polydomain nematic elastomers turns locally into the shear in each domain across the nematic axis (see Fig. 2). This effect is similar to stripe formation in a monodomain nematic elastomer under uniaxial extension across the nematic director [36,37]. In that case, at a critical stress controlled by the boundary conditions, the sample breaks into series of parallel stripes. The uniaxial deformation turns into a shear in stripes with shear direction alternating from stripe to stripe. The deformation becomes hard again when the director completes a 90° rotation. As the sample is clamped at both ends it imposes boundary conditions on the system and together with the sample geometry sets the value of the critical stress. Similar effects may also be important in the case of *P-M* transition and may account for the facts that sometimes the threshold stress is temperature independent and the sample sometimes is not absolutely soft through the transition.

At and past the transition the characteristic domain size ξ_D changes only weakly with applied stress and, therefore, the increase in the long-range order takes place via the reorientation of individual correlated regions, rather than through domain growth. Due to the rubber-elastic energy, the domain boundaries sharpen on increasing field and are left in the system as ''fossils'' even after the complete alignment between all domains is achieved. This is again similar to monodomain nematic elastomer with stripes, where after the completion of the transition the director has a zig-zag configuration making sharp u-turns between the neighboring stripes, now having the director parallel to the extension axis.

Most of the features of the *P-M* transition are correctly described by the model though there are still some open questions as to why the threshold stress value may be independent on temperature and how strong is the the influence of the sample size and shape and boundary conditions (clamping) on the value of critical stress.

The theoretical model described here should be equally applicable to the magnets with weak random disorder aligned by an external magnetic field. The main difference is the absence of the effect of elastic domain wall localisation (which was the main factor in creating the threshold stress σ_c in elastomers). The value of the remaining threshold magnetic field is predicted to be small and lies in the magnetic field range not usually covered experimentally. However the results of the renormalization group technique contradict the predictions of our model and show no evidence of the discontinuous transition in random magnets in the external field [38]. Thus the applicability of the model to magnetic systems remains an open question. As only the replica symmetric solution above the threshold was considered, our model does not give any answer to the question of how the correlations in the system are changed below the *P-M* transition and whether there is any long range order at this stage.

One of the possible direct applications of the model is in nematic polymers for nonlinear optics [39]. These materials possess strong dipolar moments along the axes of the mesogenic groups which are tailored head to tail on polymer chains. This allows for imposing the dipolar order (necessary to reveal the nonlinear optical properties) by poling the system in the external electric field. Nematic polymers are normally in the polydomain state and the dipolar order is coupled with nematic quadrupolar ordering. Thus to achieve a high degree of dipolar order it will be necessary to apply an electric field above the critical value and to pass through the *P-M* transition. To describe the equilibrium and dynamic properties of such a system under the influence of the electric field is an interesting and appealing problem. The role of random disorder effects is also relevant in the analysis of slow dynamics of relaxation in nematic elastomers.

ACKNOWLEDGMENTS

This work was supported by EPSRC. We appreciate many valuable discussions with P.D. Olmsted and M. Warner, the access to the experimental data of H. Finkelmann, C. Ortiz, R.V. Talroze, and S.M. Clarke, and critical remarks of T. Emig.

[1] *Handbook of Liquid Crystals*, Vol. 3, edited by D. Demus, J. Goodby, G. W. Gray, H.-W. Spiess, and V. Voll (Wiley-VCH, Weinheim—Chichester, 1998).
[2] I. Chuang, R. Durrer, N. Turok, and B. Yurke, Science **251**, 1336 (1991).
[3] T. Bellini, N. A. Clark, C. D. Muzny, L. Wu, C. W. Garland, D. W. Schaefer, and B. J. Oliver, Phys. Rev. Lett. **69**, 788 (1992).
[4] D. K. Yang, L-C. Chien, and J. W. Doanne, Appl. Phys. Lett. **60**, 3102 (1992).
[5] A. I. Larkin, Zh. Éksp. Teor. Fiz. **58**, 1466 (1970) [Sov. Phys. JETP **31**, 784 (1970)].
[6] Y. Imry and S.-K. Ma, Phys. Rev. Lett. **35**, 1399 (1975).
[7] M. Čopič and A. Mertelj, Phys. Rev. Lett. **80**, 1449 (1998).
[8] S. M. Clarke and E. M. Terentjev, Phys. Rev. Lett. **81**, 4436 (1998).
[9] A. ten Bosch and L. Varichon, Macromol. Theory Simul. **3**, 533 (1994).
[10] J. Schätzle, W. Kaufhold, and H. Finkelmann, Macromol. Chem. Phys. **190**, 3269 (1989).
[11] J. Küpfer and H. Finkelmann, Macromol. Chem. Phys. **195**, 1353 (1994).
[12] R. V. Talrose, N. A. Plate, and E. R. Zubarev *et al.*, Polym. Sci. U.S.S.R. **39**, 41 (1997); [Vysokomol. Soedin. Ser. A Ser. B **39**, 63 (1997).
[13] E. R. Zubarev, R. V. Talrose, T. I. Yuranova, N. A. Plate, and H. Finkelmann, Macromolecules **31**, 3566 (1998).
[14] C. Ortiz, R. Kim, E. Rodigheiro, C. K. Ober, and E. J. Kramer, Macromolecules **31**, 4074 (1998).
[15] C. Ortiz, C. K. Ober, and E. J. Kramer, Polymer **39**, 3713 (1998).
[16] C. Ortiz, M. Wagner, N. Bhargava, C. K. Ober, and E. J. Kramer, Macromolecules **31**, 8531 (1998).
[17] S. M. Clarke, E. Nishikawa, H. Finkelmann, and E. M. Terentjev, Macromol. Chem. Phys. **198**, 3485 (1997).
[18] S. M. Clarke, E. M. Terentjev, I. Kundler, and H. Finkelman, Macromolecules **31**, 4862 (1998).
[19] E. M. Chudnovskij and R. A. Serota, Phys. Rev. B **26**, 2697 (1982).
[20] S. F. Edwards and M. Mutukumar, J. Chem. Phys. **89**, 2435 (1988).
[21] M. Warner and E. M. Terentjev, Prog. Polym. Sci. **21**, 853 (1996).
[22] M. Warner, P. Bladon, and E. M. Terentjev, J. Phys. II **4**, 93 (1994).
[23] P. D. Olmsted, J. Phys. II **4**, 2215 (1994).
[24] P. G. de Gennes, in *Liquid Crystals of One- and Two-Dimensional Order*, edited by W. Helfrich and G. Heppke (Springer, Berlin, 1980), p. 231.
[25] P. G. de Gennes, C. R. Seances Acad. Sci., Ser. B **281**, 101 (1975).
[26] W. Kaufhold, H. Finkelmann, and H. R. Brand, Macromol. Chem. Phys. **192**, 2555 (1991).
[27] A. Halperin, J. Chem. Phys., **85**, 1081 (1986).
[28] N. Uchida and A. Onuki, Europhys. Lett. **45**, 341 (1999).
[29] S. V. Fridrikh and E. M. Terentjev, Phys. Rev. Lett. **79**, 4661 (1997).
[30] S. F. Edwards and P. W. Anderson, J. Phys. F **5**, 965 (1975).
[31] M. Mezard and G. Parisi, J. Phys. I **1**, 809 (1991).
[32] T. Giamarchi and P. Le Doussal, Phys. Rev. Lett. **72**, 1530 (1994); Phys. Rev. B **52**, 1242 (1995).

[33] X. D'Allest *et al.*, Phys. Rev. Lett. **61**, 2562 (1988).
[34] I. Kundler and H. Finkelmann, Macromol. Chem. Phys. **199**, 677 (1998).
[35] P. G. de Gennes and J. Prost, *The Physics of Liquid Crystals* (Clarendon Press, Oxford, 1995).
[36] I. Kundler and H. Finkelmann, Macromol. Chem. Rapid Commun. **16**, 679 (1995).
[37] G. C. Verwey, M. Warner, and E. M. Terentjev, J. Phys. II **6**, 1273 (1996).
[38] T. Emig and T. Natterman, Phys. Rev. Lett. **79**, 5090 (1997).
[39] C. Heldmann and M. Warner, Macromolecules **31**, 3519 (1998).